ARTICLE

Photophysical Properties of 4′-(*p*-aminophenyl)-2,2′:6′,2″-terpyridine

Peng Song[a], Shi-guo Sun[b], Pan-wang Zhou[a], Jian-yong Liu[a*], Yong-qian Xu[b], Xiao-jun Peng[b*]

a. State Key Laboratory of Molecular Reaction Dynamics, Dalian Institute of Chemical Physics, Chinese Academy of Science, Dalian 116023, China
b. State Key Laboratory of Fine Chemicals, Dalian University of Technology, Dalian 116012, China

(Dated: Received on May 4, 2010; Accepted on May 19, 2010)

Spectral and photophysical investigations of 4′-(*p*-aminophenyl)-2,2′:6′,2″-terpyridine (APT) have been performed in various solvents with different polarity and hydrogen-bonding ability. The emission spectra of APT are found to exhibit dual fluorescence in polar solvents, which attributes to the local excited and intramolecular charge transfer states, respectively. The two-state model is proven out for APT in polar solvent by the time-correlated single photon counting emission decay measurement. Interestingly, the linear relationships of different emission maxima and solvent polarity parameter are found for APT in protic and aprotic solvents, because of the hydrogen bond formation between APT and alcohols at the amino nitrogen N25. Furthermore, the effects of the complexation of the metal ion with tpy group of APT and the hydrogen bond formation between APT with methanol at the terpyridine nitrogen N4−N8−N14 are also presented. The appearance of new long-wave absorption and fluorescence bands indicates that a new ground state of the complexes is formed.

Key words: Dual fluorescence, Local excited state, Intramolecular charge transfer, Terpyridine, Complexation, Fluorescence decay

I. INTRODUCTION

4-(dimethyl-amino)benzonitrile (DMABN), as a model, has been studied experimentally and theoretically [1−3], since the first observation of the dual fluorescence phenomenon around 1960 by Lippert *et al.* [4], and dual fluorescence has been observed for numbers of donor(D)/acceptor(A) molecules [5−8]. Rettig *et al.* have shown that the ratio of the long-wavelength to the short-wavelength fluorescence depends on the type of the $-NR_2$ substituent [9]. For the first time, 2,3,5,6-tetrafluoro-4-aminobenzonitrile (ABN4F), the electron donor/acceptor molecule with an NH_2 group, is observed to exhibit intramolecular charge transfer (ICT) fluorescence, and the ICT state of its analogue, 2,3,5,6-tetrafluoro-4-(dimethylamino)benzonitrile (DMABN4F), has a dipole moment of around 14 D, clearly smaller than that of DMABN (17 D). This difference is attributed to the electron withdrawing from the CN group to the phenyl ring, exerted by the four F-substituents [10]. Otherwise, with phenyl-substituted 2,2′:6′,2″-terpyridines, for example, the dipole moment increases from the electronic ground state (μ_g) via 2 D to the local excited (LE) state (μ_e(LE)) [11], but in the case of N-alkyl and N-phenyl derivatives of 6-amino- and 6,6′-diamino-2,2′:6′,2″-terpyridines, the $\Delta\mu$ is determined to be 10 D for the difference between the ground and ICT state [12]. Unfortunately, dual-fluorescence has not been reported for these systems.

In the investigation of D/A-systems with ICT character, the molecular structure of the ICT state is an important point of discussion. It is now well-established that this process is an intramolecular phenomenon and that the local excited and ICT states are structural conformers [13]. A controversy still exists, however, concerning the molecular structure of the ICT state, named the twisted intramolecular charge transfer (TICT) and the planar intramolecular charge transfer (PICT). For example, in the TICT model of DMABN [1, 14], the dimethylamino group is expected to be perpendicular to the plane of the phenyl ring; while in the PICT model the two halves coplanar to each other [15]. Recently, Haas *et al.* have studied the dual fluorescence of DMABN and other benzene derivatives through theoretical calculation, and concluded that the origin of the dual fluorescence could be explained by a charge transfer model based on the properties of the benzene anion radical, which classified the CT states as quinoid (Q) and antiquinoid (AQ) forms [16]. The three low-lying electronically excited states are expected for these molecules, in general, two of which are of CT character, whereas the third is a LE state. Dual fluorescence may arise from any two of these states, as each has a different geometry at which it attains a minimum energy. As an example, if the dipole moment is larger in the perpendicular geometry than that in the planar one, this

*Authors to whom correspondence should be addressed. E-mail: beam@dicp.ac.cn, pengxj@dlut.edu.cn

geometry is preferred in polar solvents, supporting the TICT model, vice versa.

On the other hand, according to our previous study [2, 17−19], the hydrogen bond (HB) in protic solvents can lead to complicated interactions, which may significantly influence the ICT state. Zhao and Han theoretically investigated for the first time the hydrogen-bonded TICT excited state of DMABN in alcoholic solvents and reassigned the infrared spectra [2]. Similar results are also observed for the pyridine group of these systems in coordination to the metal ion. But the protonation effects on the excited-state electron transfer are found to be very different from the neutral complexes (such as HB). New, highly fluorescent terpyridines, which respond to zinc ions with a large red-shift and an enhancement in emission, have been reported to be fluorescence sensors, using ICT mechanics [20, 21]. As a new class of potential fluorescence sensor, the different substituent of terpyridines with its ascendant coordination capability with transition metal ions, has get more attention to its photophysical and photochemical properties studies.

In this work, we investigate the dual fluorescence of APT in polar solvents. Also the effects of HB formed between APT and alcohols at different position and the complexation of transition metal ion Zn^{2+} with APT are studied. With the steady-state spectra and the fluorescence decay measured by the TCSPC method, we present the photophysical properties of APT.

II. EXPERIMENTS

A. Molecules and solvents

APT was synthesized and purified by reaction of 2-acetylpyridine, *p*-nitrobenzaldehyde, and solid NaOH, which was discussed detailedly in Ref.[22]. We obtained the desired compound in 62% yield, and the structural formulas of the APT molecule is shown in Fig.1. The solute APT dissolved in *n*-hexane (HEX), *n*-heptane, 1,4-dioxane, toluene, ethylether, tetrahydrofuran (THF), dichloromethane, *n*-hexanol, *n*-butanol, *n*-propanol, acetone, ethanol, and acetonitrile (MeCN) at room temperature (21 °C).

B. Absorption/fluorescence and fluorescence decays spectra

Each metal ion titration experiment was started with a 3 mL acetonitrile solution with a known concentration (about 0.1 mmol/L). Solutions (1 mmol/L) of metal salt in deionized water were used for the titration. Buffer solutions (pH=7.0) were prepared using 0.03 mol/L HEPES. A 10 μL aliquot of the salt solution was added each time to the APT solution and the solution was stirred constantly during the titration and the steady-state spectra were measured 10 min after each addition of the metal ion. The steady-state absorption spectra were run on a UV-visible absorption spectrophotometer (HP8453, Hewlett-Packard Corp). The fluorescence spectra were measured with a FluoroMax-4P Spectrofluorometer (HORIBA JOBIN YVON Corp). The fluorescence decay time was obtained with a nanosecond laser (λ_{exc}=295 nm) time-correlated single photon counting (TCSPC) setup. The instrument response function of the laser SPC system has a full width at half maximum (FWHM) of 1 ns and the time resolution is estimated at 200 ps. The time ranges are 55 ps/channel, in 4096 effective channels. The estimated reproducibility is around 2% for the nanosecond decays. The fluorescence decay data are fitted to the exponentials function using a least-squares algorithm with the commercial IBH software.

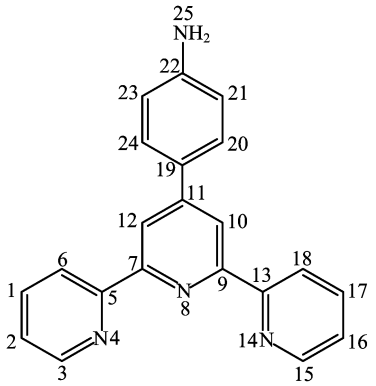

FIG. 1 Structural formula of the APT molecule.

III. RESULTS AND DISCUSSION

For comparison, the absorption and fluorescence spectra of APT in MeCN and *n*-hexane are shown in Fig.2. The near-UV absorption spectra of APT show a shoulder in the low-energy part of the spectrum and a dominant band centered at about 35200 cm^{-1} in *n*-hexane and MeCN. The predominant absorption spectrum is observed to be independent of the solvent polarity, which indicates that the ground state and the Franck-Condon (FC) excited state have similar dipole moment. The fluorescence spectra of APT in *n*-hexane and MeCN at room temperature are similar to those of DMABN. In MeCN, the fluorescence spectrum consists of two components: a minor LE emission with a maximum at 26041 cm^{-1}, and a predominant red-shift ICT band peaking at 19443 cm^{-1} (see Table I), and the fluorescence quantum yield ratio ϕ'(ICT)/ϕ(LE) between these two bands is observed to be 9.51. In addition, the fluorescence spectrum is also found to be changed with the excitation wavelength λ_{exc}, which displays that the ratio ϕ'(ICT)/ϕ(LE) apparently decreasing when λ_{exc} becomes shorter. This wavelength dependence is attributed to the distribution of the N-phenyl twist an-

DOI:10.1088/1674-0068/23/05/558-564

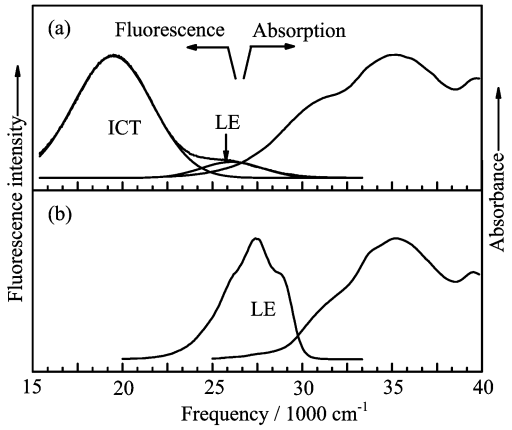

FIG. 2 Normalized fluorescence and absorption spectra of APT (a) in MeCN and (b) in *n*-hexane at room temperature. Excitation wavelength λ_{exc}=286 nm.

TABLE I Data for APT in MeCN or in *n*-hexane (HEX) when indicated[a].

ν^{max}(ICT)/cm^{-1}	19443
ν^{max}(LE)/cm^{-1}	26041
(HEX) ν^{max}(LE)/cm^{-1}	27397
ϕ'(ICT)+ϕ(LE)	0.13[b]
ϕ'(ICT)/ϕ(LE)	9.51
$E(S_1)$/cm^{-1}[c]	26614
(HEX) $E(S_1)$/cm^{-1}	29762

[a] ν^{max}(ICT) and ν^{max}(LE) are fluorescence maximum, ϕ'(ICT) and ϕ(LE) are fluorescence quantum yields, $E(S_1)$ is energy of the S_1 state.
[b] Data from Ref.[10] in dichloromethane.
[c] Energy of the crossing of the normalized absorption and fluorescence spectra.

gle in the ground state [6, 23], and confirm that a two-state model is appropriate for describing the photoluminescence (PL) spectra of APT in polar solvent. While in non-polar solvent, such as *n*-hexane, the APT is found to exhibit only LE emission with the maximum at 27397 cm^{-1}.

A. The hydrogen-bonding effects on the APT molecule

It has been well shown that protic solvents, complexation with Zn^{2+} and protonation effects would affect the spectroscopic and photophysical properties of the compound. Similar behaviors have been found for APT molecule, which can be easily seen from the absorption and fluorescence spectra (at room temperature) of APT in aprotic, protic solvents and 1:1 complexes with Zn^{2+} in MeCN. In bulk alcohol the formation of various specific complexes is expected. From Fig.3, the red shift of the lower-energy absorption bands in alcoholic solvents (ethanol as the example) with respect to that in

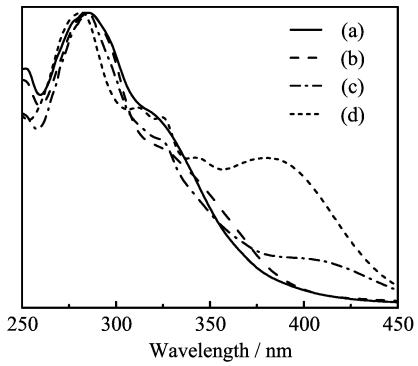

FIG. 3 Normalized absorption spectra of APT in (a) MeCN, (b) ethanol, (c) methanol, and (d) 1:1 complexes with Zn^{2+} in MeCN.

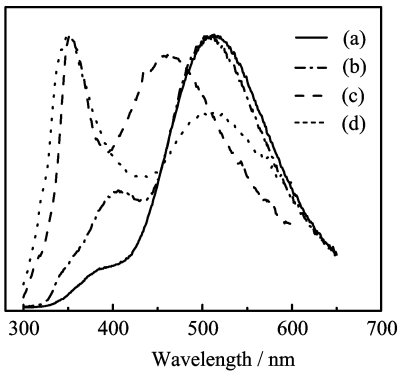

FIG. 4 Normalized fluorescence spectra of APT in (a) MeCN, (b) ethanol, (c) methanol, and (d) 1:1 complexes with Zn^{2+} in MeCN, excited by λ_{exc}=286 nm.

MeCN, suggests that most of these species correspond to the complexes hydrogen bonded at the side chain amino nitrogen N25. HB at the terpyridine nitrogen N4−N8−N14 can only formed with methanol, the hydrogen donor ability α=0.93 is much larger than other alcohols, vide infra. And the fluorescence spectra are also observed to show strong solvatochromic red-shift in protic solvents, which can be easily seen from Fig.4 that the fluorescence maximum of APT in ethanol (ε=24.55) is almost similar to that in MeCN (ε=37.5). Another type of HB is also possible to be formed mostly, which include the participation of the amino hydrogen with hydrogen-bonding solvents. This has been proven by our previous experimental and theoretical calculations, and the results suggest that this type of HB is enhanced at the TICT excited-state of 7-aminocoumarin [18].

As known that, the strong hydrogen-bond donating and accepting solvents (such as alcohols) are expected to stabilize the chromophoric molecules by the specific solute-solvent hydrogen-bonding interactions, and affect the property of the excited-state, which would result in the different ν^{max}_{fluo}-$f(\varepsilon, n)$ linear relationship and the different dipole moment change $\Delta\mu$ of the first excited-state between alcoholic solvents and aprotic sol-

DOI:10.1088/1674-0068/23/05/558-564

TABLE II Fluorescence decays of APT in *n*-hexane, MeCN, and MeCN in the presence zinc ions measured by TCSPC setup.

Solvent		A_1	τ_1/ns	A_2	τ_2/ns
n-hexane[a]		0.072±0.0002	2.36±0.006		
MeCN	LE	0.006±0.0004	4.72±0.036	0.186±0.0007	0.36±0.006
	ICT	0.067±0.0001	3.79±0.007	−0.070±0.0009	0.20±0.013
MeCN-Zn[b]	LE	0.006±0.0003	5.18±0.037	0.207±0.0008	0.30±0.006
	ICT	0.065±0.0001	4.36±0.008	−0.077±0.0010	0.18±0.020

[a] Single exponential decay.
[b] 1:1 complexes with Zn^{2+} in MeCN.

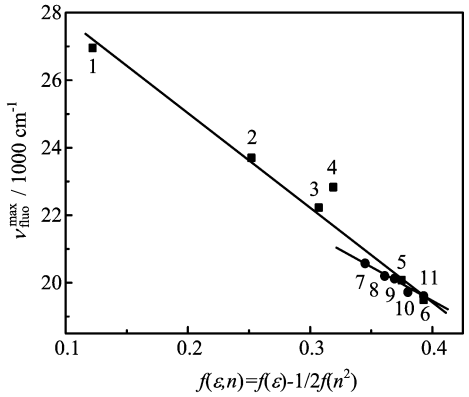

FIG. 5 Plot of the emission maxima $\nu_{\rm fluo}^{\rm max}$ of APT as a function of solvent polarity parameter $\Delta f(\varepsilon, n)$. Solvent: 1 1,4-dioxane, 2 ethylether, 3 THF, 4 dichloromethane, 5 acetone, 6 acetonitrile, 7 *n*-hexanol, 8 *n*-butanol, 9 *n*-propanol, 10 ethanol, and 11 methanol.

vents [24, 25].

Using the Lippert-Mataga equation [26], the maxima $\nu_{\rm fluo}$ of the fluorescence bands of APT are plotted against the polarity parameter $f(\varepsilon, n)=f(\varepsilon)-1/2f(n^2)$, as shown in Fig.5, in various polarities and hydrogen bonding abilities, namely, *n*-hexane (nonpolar), acetonitrile (polar but aprotic), methanol and ethanol (polar as well as protic), and so on. The Onsagar cavity radius ρ is estimated to be 4.09 Å, by applying the partial volume addition method, as suggested by Edward [27]. The theoretical value of $\mu_{\rm g}$, which is calculated, is 5.3 D [28, 29]. From the Fig.5, we can see that the solvatofluorochromic slopes (m_f) of APT exhibits different linear relationship between the alcoholic and aprotic solvents. Then we get the first excited-state dipole moments to be 17.3 and 16.7 D for APT in aprotic and alcoholic solvents, respectively, which reveals a larger charge-transfer character of the first excited state relative to that of the ground state in both kinds of solvents. In addition, the different $\nu_{\rm fluo}^{\rm max}$-$f(\varepsilon, n)$ linear relationship between the alcoholic and aprotic solvents, however, indicates that the polarity of the solvent is not the exclusive parameter to determine the excited-state dipole moment. Hydrogen bond, as the electrostatic interaction between the solute and solvent, is also a key factor to affect the character of the excited-state [30, 31]. Zhao *et al.* has systematically investigated the excited-state hydrogen bonding dynamics and demonstrated that intermolecular hydrogen bonding formed between chromophores and solvents can be significantly strengthened or weakened in electronically excited states and has a remarkable influence on the excited-state processes of organic and biological chromophores in solution and gas phase [30−34]. And this also supports the formation of HB in this excited-state, which is expected to be a TICT state most possibly.

B. Metal ion complexometric effects and the position of the HB formed with APT in alcohols

Terpyridines (tpy) are well-known to show good affinity for Zn^{2+}, and the binding of Zn^{2+} always leads to spectral changes due to the formation of complexes [20, 21]. These effects on our APT-Zn^{2+} complexes are investigated by spectrophotometric experiments, in which the metal ions are coordinated in the tpy site of APT in MeCN-HEPES (9:1, pH=7.0) with 1:1 equivalent proportion, and the steady-state absorption and fluorescence spectra are much distinguishable from those in the other selected solvents (except for methanol) in Fig.3 and Fig.4. Ionochromic effects in the optical absorption spectra of metalated complexes are illustrated in Fig.3. Several spectral characteristics are depicted: (i) Zn^{2+} binding do not cause large shift of the absorption maximum peak relative to that in the metal-free molecule, (ii) a new absorption band (peaking at about 385 nm) appears at lower energies in the presence of Zn^{2+}. Chen *et al.*, have stated that conjugated systems in solution can be viewed as an ensemble of the segments of different conjugation lengths, which are responsible for their optical absorption peaks. When metal ions are chelated to the molecule, the lengths of conjugated segments are changed [35]. Therefore the appearance of a new absorption band of the APT in the presence Zn^{2+} indicates that there is an interaction between the metal ion and the tpy site, and the complex of Zn^{2+} and APT is formed in the ground state. The complex-

DOI:10.1088/1674-0068/23/05/558-564

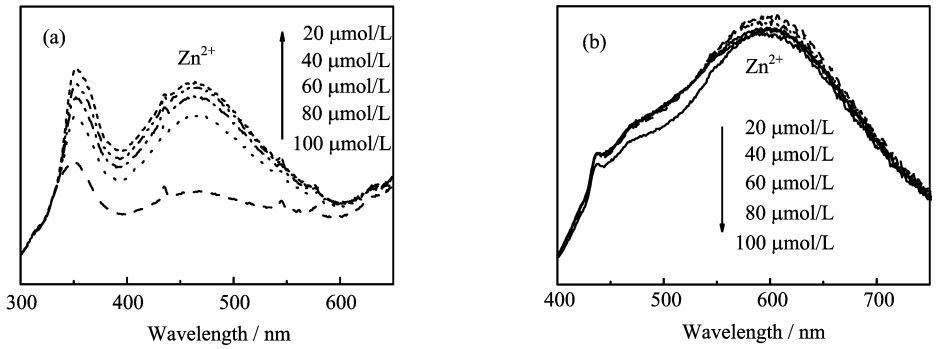

FIG. 6 Fluorescence spectra of APT in the presence of Zn^{2+} in MeCN, excited at 286 nm (a) and 385 nm (b), the arrows indicate the direction of the change as metal ion were added.

ation of Zn^{2+} and APT can also be deduced from the fluorescent spectra. When excited at 385 nm, the metal-free APT in MeCN shows a relative strong fluorescence with its unchanged maximum as compared with the ICT state with 286 nm excitation. But the ion binding complex, with the same excitation, exhibits strong fluorescence with the maximum at about 600 nm (Fig.6(b)). Also, the conformational change of terpyridine part of the APT-Zn^{2+} complex would result in the modification of the whole conjugate structure of the complexes, and the ICT emission from the conjugation-dependent structure of the whole system would be changed, accordingly. Therefore, the fluorescence (about 600 nm) comes from the whole APT-Zn^{2+} complex.

The steady-state absorption and fluorescence spectra (Fig.3 and Fig.6) results also indicate that the APT-Zn^{2+} complex in MeCN has two distinguishable emitting species that can be preferentially excited by different λ_{exc}. Although the absorption and emission of the Zn^{2+}-bound segments of the system have lower energies compared to their counterpart of the metal-free segments (π_{tpy}-π^*_{tpy}, and unaffected by introducing Zn^{2+}), the PL originated from the metal-free segments is not quenched due to the energy flow to the Zn^{2+}-occupied segments. The two chemically different species emit independently with little interaction between each other [35]. On the other hand, as we can see from Fig.4 and Fig.6(a), the LE and ICT state fluorescence maxima of APT-Zn^{2+} complexes blue shift to 350 and 465 nm, respectively, when excited at 286 nm. As discussed by Araki *et al.* [11], the 4′-phenyl-terpyridine has almost the same absorption and fluorescence spectra as those of terpyridine itself. Once the electron donor $-NH_2$ or $-NMe_2$ are introduced into the system, a new lower-energy absorption band appears, and the fluorescence spectra exhibit dramatic red shifts. Furthermore, the red-shifts become more obvious with the increasing of the donor ability. Their results also indicate that the different molecular orbits transition could be ascribed to the different absorption band. The energy excitation band of 4′-phenyl-terpyridine (about 280 nm) is a local excitation (LE) transition (π_{tpy}-π^*_{tpy}). In the case of $-NH_2$ or $-NMe_2$ substituted 4′-phenyl-terpyridine, the energy level of π_{tpy} is not much different from that of 4′-phenyl-terpyridine. So we believe that, the absorption band centered at 286 nm, corresponds to the π_{tpy}-π^*_{tpy} transition for the APT-Zn^{2+} complexes, and this transition is unaffected by introducing Zn^{2+}. With 286 nm excitation, the fluorescence mainly comes from metal-free segments of complex. And because of the coordination of the Zn^{2+} with terpyridine, the terpyridine part of the complexes is expected to be a planar structure as the terpyridine itself. Hence the emission from the LE state of the metal-free segments is more similar to that of terpyridine, which has a fluorescence maximum at about 340 nm [11]. This point of view can also be proven from Fig.6(a): this LE emission increases with the increasing concentration of Zn^{2+}.

Furthermore, the conformational change of terpyridine part of the APT-Zn^{2+} complexes would result in the reduction of the whole conjugate structure of metal-free segments of the complexes, and the ICT emission from it would be changed, accordingly. In addition, with both changes of the conjugated length and the structure of the molecule, the ICT process decreases when the APT binds with the metal ion, resulting in a simultaneous decrease of the ratio ϕ'(ICT)/ϕ(LE) [36]. Similar analysis is suitable for APT in methanol, (the hydrogen donor ability is much larger than other alcohols) when the interaction is strong enough to change the conformation of the ground state of the APT-methanol complexes, as can be seen from Fig.3. In accordance with the similarity of the fluorescence spectra for APT in methanol and APT-Zn^{2+} complexes in MeCN, when excited at 286 nm (see Fig.4), we can conclude that the strong HB is formed between APT and methanol at the terpyridine nitrogen N4−N8−N14. In addition, the red-shifts of the new appearing absorption band (Fig.3) and the lower energy emission band (ICT emission in Fig.4), relative to those of APT-Zn^{2+} complex, indicate that the HB at the amino nitrogen N25 is also formed between APT and methanol. From the analysis above, we can get the conclusion that: (i) the HB is formed at the amino nitrogen N25 for APT

DOI:10.1088/1674-0068/23/05/558-564

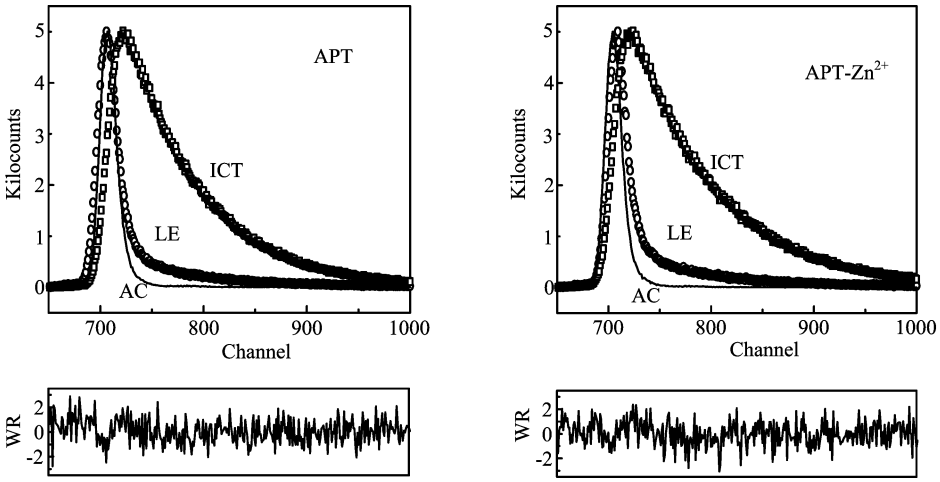

FIG. 7 Fluorescence decays at different observation wavelength of APT in MeCN (left) and APT-Zn^{2+} 1:1 complexes in MeCN (right) at room temperature. The weighted residuals (WR) and the autocorrelation functions AC are related to emission ICT. Excitation wavelength: 295 nm nanosecond laser, 55 ps/channel.

in all alcohols; (ii) the HB at the terpyridine nitrogen N4−N8−N14 can only be formed between APT and methanol, because only the HB ability of methanol is strong enough to change the structure of the terpyridine as the coordination of Zn^{2+} with terpyridine, when the complexes formed.

C. Bimodal kinetics of APT and APT-Zn^{2+} complexes in MeCN

The bimodal kinetics and the reversibility of the excited-state ICT reaction of APT and APT-Zn^{2+} in MeCN at room temperature are proven by the nanosecond fluorescence decay investigations. The typical fluorescence decay curves are presented in Fig.7, and the respective decay time constants are listed in Table II. The results, as shown below, suggest a conventional precursor-successor kinetic model is suitable for describing the dual fluorescence mechanism of APT and APT-Zn^{2+} (1:1 complex) in polar aprotic solvent, when excited by 295 nm nanosecond laser. From the emission decay data (Table II) for these two compounds, two decay times ($\tau_2 \approx 300$ ps and $\tau_1 \approx 5$ ns) are sufficient to fit the LE decay, which indicate that at room temperature the equilibrium LE↔ICT is established within 200 ps (or even shorter time range). The presence of a negative amplitude for the shortest ICT decay time τ_2 with an amplitude ratio A_{22}/A_{21} close to -1, indicates that the ICT state of APT cannot be formed by direct excitation of the ground state, similar to what has been observed with DMABN and related molecules [5]. This decay analysis of APT corresponds to that for a two-state model consisting of LE state from which an ICT state is formed after photoexcitation. The observation wavelength of the LE and ICT fluorescence bands are separated largely enough to prevent any overlap of both emissions. Whereas in *n*-hexane, the fluorescence decay of APT can only be fitted by a single exponential function. It is also found that the fluorescence decay is independent of the emission wavelength, which indicates that APT only emits from one fluorescence state, named LE state, in nonpolar solvent. It should be noted that, the growing-in component is hard to be presented exactly for the ICT fluorescence decay, which is mainly due to the time-resolved limit of our nanosecond time resolved TCSPT setup (55 ps/channel). More detailed studies are needed by the picosecond (or even femtosecond) time resolved spectra results. In addition, the lifetime increases with addition of Zn^{2+}, which can contribute to the greater rigidity of the zinc complexes and then reduce the efficacy with which C−C stretching vibrations are able to act as energy accepting modes for deactivation of the excited state [20].

IV. CONCLUSION

We have measured the photophysical properties of APT molecule. The emission spectra are found to exhibit dual fluorescence in polar aprotic solvent, such as acetonitrile, which can be attributed to the LE and ICT state, respectively. The maxima $\nu_{\rm fluo}$ of the fluorescence bands are plotted against the polarity parameter in aprotic/protic solvents, and both of them result in larger dipole moment (17.3 and 16.7 D, respectively), which reveals an ICT character in the excited state. The different $\nu_{\rm fluo}^{\rm max}$-$f(\varepsilon, n)$ linear relationship caused by HB effects of the alcoholic solvents informs the HB formation between APT and alcohols at the amino nitrogen N25 or/and the participation of the amino hydrogen with hydrogen-bonding solvents. In addition, our experimental results and analyses have shown that a new specie is formed for APT in methanol and APT-Zn^{2+}

DOI:10.1088/1674-0068/23/05/558-564

complexes in the ground state, because of the appearance of a new long-wave absorption band, and once excited at this energy the complexes show an additional fluorescent band peaking at lower energy range. This indicates that the coordination of the metal ion with tpy group and HB formation between APT with methanol at the terpyridine nitrogen N4−N8−N14, which result in the change of absorption and photoluminescence spectra. Finally, the results, supported by the fluorescence decay measurement on LE and ICT emission bands separately, suggest that the two-state model is appropriate for describing the dual fluorescence spectra of APT in polar solvent.

V. ACKNOWLEDGMENTS

This work was supported by the National Natural Science Foundation of China (No.20973168 and No.20633070), the Solar Energy Initiative of the Knowledge Innovation Program of the Chinese Academy of Sciences (No.KGCX2-YW-394-2), and the National Key Basic Research Special Foundation of China (No.2009CB220010).

[1] Z. R. Grabowski, K. Rotkiewicz, and W. Rettig, Chem. Rev. **103**, 3899 (2003).
[2] G. J. Zhao and K. L. Han, J. Comput. Chem. **29**, 2010 (2008).
[3] X. F. Xu, Z. X. Cao, and Q. E. Zhang, J. Chem. Phys. **122**, 194305 (2005).
[4] W. L. E. Lippert, F. Moll, W. Nägele, H. Boos, H. Prigge, and I. Seibold-Blankenstein, Angew. Chem. **73**, 695 (1961).
[5] S. Techert and K. A. Zachariasse, J. Am. Chem. Soc. **126**, 5593 (2004).
[6] T. Yoshihara, S. I. Druzhinin, A. Demeter, N. Kocher, D. Stalke, and K. A. Zachariasse, J. Phys. Chem. A **109**, 1497 (2005).
[7] M. T. Sun, Chem. Phys. Lett. **408**, 128 (2005).
[8] G. J. Zhao, B. H. Northrop, P. J. Stang, and K. L. Han, J. Phys. Chem. A **114**, 3418 (2010).
[9] W. Rettig, J. Lumin. **26**, 21 (1981).
[10] V. A. Galievsky, S. I. Druzhinin, A. Demeter, Y. B. Jiang, S. A. Kovalenko, L. P. Lustres, K. Venugopal, N. P. Ernsting, X. Allonas, M. Noltemeyer, R. Machinek, and K. A. Zachariasse, ChemPhysChem **6**, 2307 (2005).
[11] T. Mutai, J. D. Cheon, S. Arita, and K. Araki, J. Chem. Soc. Perkin Trans. **27**, 1045 (2001).
[12] J. D. Cheon, T. Mutai, and K. Araki, Org. Biomol. Chem. **5**, 2762 (2007).
[13] T. Yoshihara, S. I. Druzhinin, and K. A. Zachariasse, J. Am. Chem. Soc. **126**, 8535 (2004).
[14] W. Rettig, B. Bliss, and K. Dirnberger, Chem. Phys. Lett. **305**, 8 (1999).
[15] K. A. Zachariasse, Chem. Phys. Lett. **320**, 8 (2000).
[16] S. Cogan, S. Zilberg, and Y. Haas, J. Am. Chem. Soc. **128**, 3335 (2006).
[17] T. S. Chu, Y. Zhang, and K. L. Han, Int. Rev. Phys. Chem. **25**, 201 (2006).
[18] P. W. Zhou, P. Song, J. Y. Liu, K. L. Han, and G. Z. He, Phys. Chem. Chem. Phys. **11**, 9440 (2009).
[19] G. J. Zhao and K. L. Han, Biophys. J. **94**, 38 (2008).
[20] W. Goodall and J. A. Gareth Williams, Chem. Commun. 2514 (2001).
[21] X. J. Peng, Y. Q. Xu, S. G. Sun, Y. K. Wu, and J. L. Fan, Org. Biomol. Chem. **5**, 226 (2007).
[22] Y. Q. Xu, *Ph.D. Dissertation*, Dalian: Dalian University of Technology, No.10207062, (2006).
[23] A. Sarkar and S. Chakravorti, Chem. Phys. Lett. **235**, 195 (1995).
[24] V. S. Pavlovich, Biopolymers **82**, 435 (2006).
[25] T. S. Singh and S. Mitra, J. Lumin. **127**, 508 (2007).
[26] E. Lippert and Z. Naturforsch, Phys. Sci. **10**, 541 (1955).
[27] J. T. Edward, J. Chem. Edu. **47**, 261 (1970).
[28] G. J. Zhao, R. K. Chen, M. T. Sun, J. Y. Liu, G. Y. Li, Y. L. Gao, K. L. Han, X. C. Yang, and L. C. Sun, Chem. Eur. J. **14**, 6935 (2008).
[29] G. J. Zhao and K. L. Han, J. Phys. Chem. A **113**, 4788 (2009).
[30] G. J. Zhao and K. L. Han, J. Phys. Chem. A **111**, 2469 (2007).
[31] G. J. Zhao and K. L. Han, J. Phys. Chem. A **111**, 9218 (2007).
[32] K. L. Han and G. Z. He, J. Photochem. Photobiol. C **8**, 55 (2007).
[33] G. J. Zhao and K. L. Han, ChemPhysChem **9**, 1842 (2008).
[34] G. J. Zhao and K. L. Han, J. Phys. Chem. A **113**, 14329 (2009).
[35] L. X. Chen, W. J. H. Jäger, D. J. Gosztola, M. P. Niemczyk, and M. R. Wasielewski, J. Phys. Chem. B **104**, 1950 (2000).
[36] V. Thiagarajan, C. Selvaraju, E. J. P. Malar, and P. Ramamurthy, ChemPhysChem **5**, 1200 (2004).

DOI:10.1088/1674-0068/23/05/558-564